

Supplementary Materials

Formic Acid Generation from CO₂ Reduction by MOF-253 Coordinated Transition Metal Complexes: A Computational Chemistry Perspective

Meng-Chi Hsieh, Ranganathan Krishnan, Ming-Kang Tsai^{*}

Department of Chemistry, National Taiwan Normal University, Taipei, 11677, Taiwan

Email: mktsai@ntnu.edu.tw

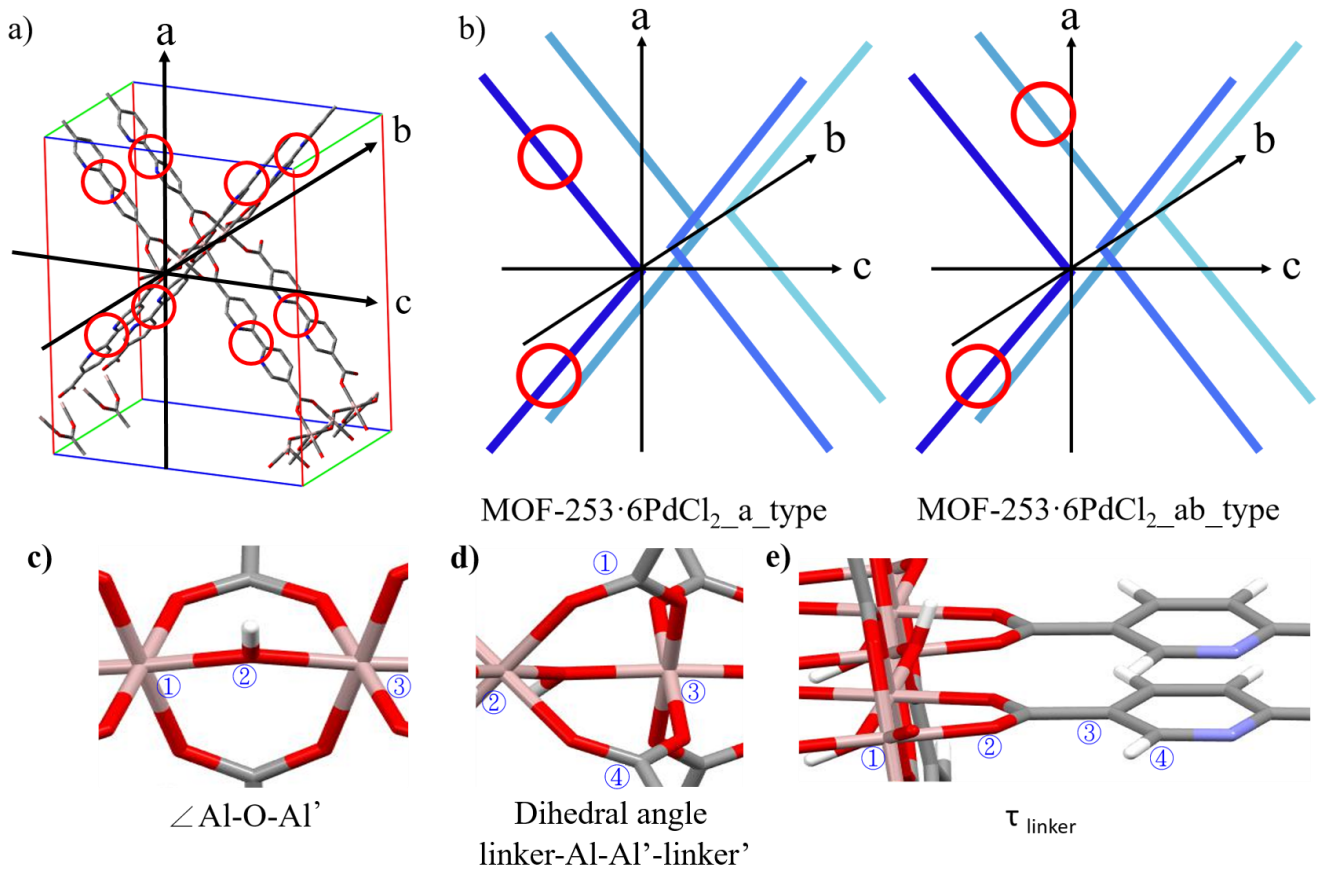


Figure S1. (a) Optimized MOF-253 using experimental lattice constants. (b) The schematic diagram of MOF-253·6PdCl₂ with the different empty sites. The red circles are the free coordination site on the linkers. (c) Al–O–Al bending angle, (d) dihedral angle of linker-Al-Al’-linker’, and (e) the rotation angle of bpy fragment (τ_{linker}) are the structure information of the MOF-253 model.

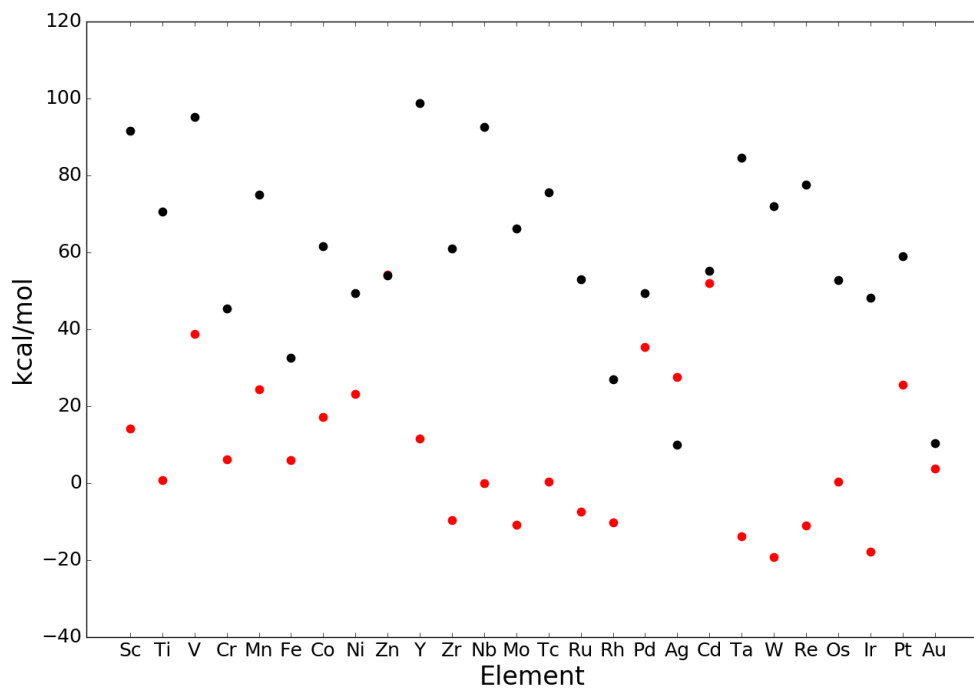


Figure S2. Energetic comparison between H atom transfer (red dot) and Cl atom transfer (black dot) from low-spin LMH_2Cl_2 complexes

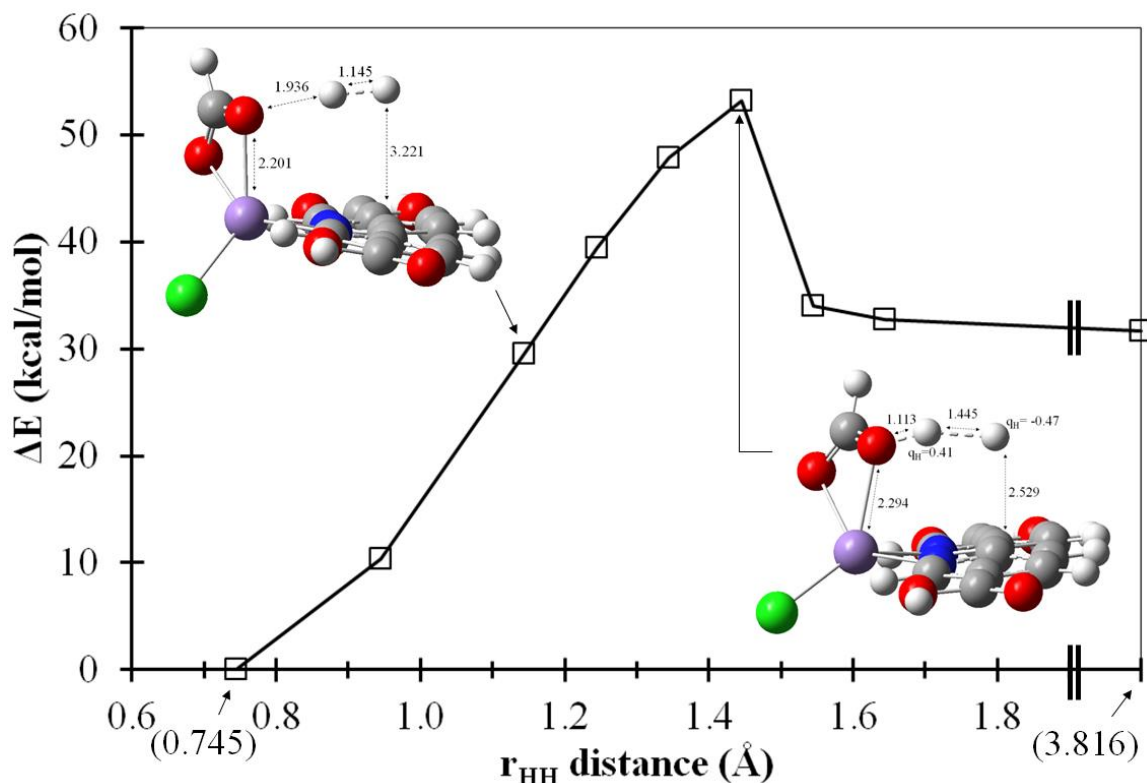


Figure S3. The calculated energetics of constrained optimization along H–H interatomic distance of LMnCl(HCO₂)(H₂) complex. The qH notation represents the atomic charge predicted by Natural Population Analysis.

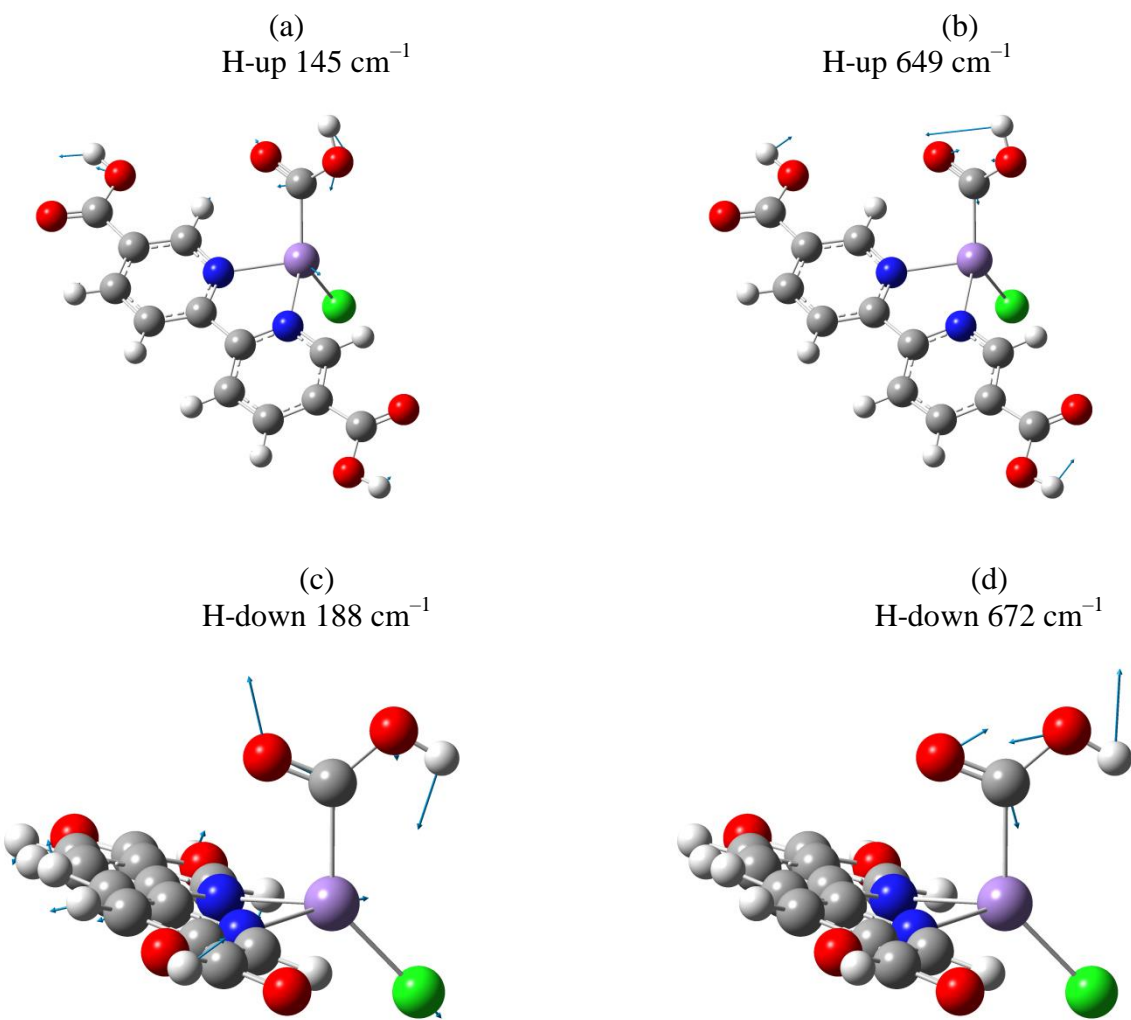


Figure S4. The identified vibrational modes of $\text{LMnCl}(\text{COOH})$ minimum structures (H-up and H-down) weaken the interactions between Mn and COOH. The arrows denote the qualitative atomic displacements. The H-up minimum is predicted to be 2.6 kcal/mol lower in energy than H-down case.

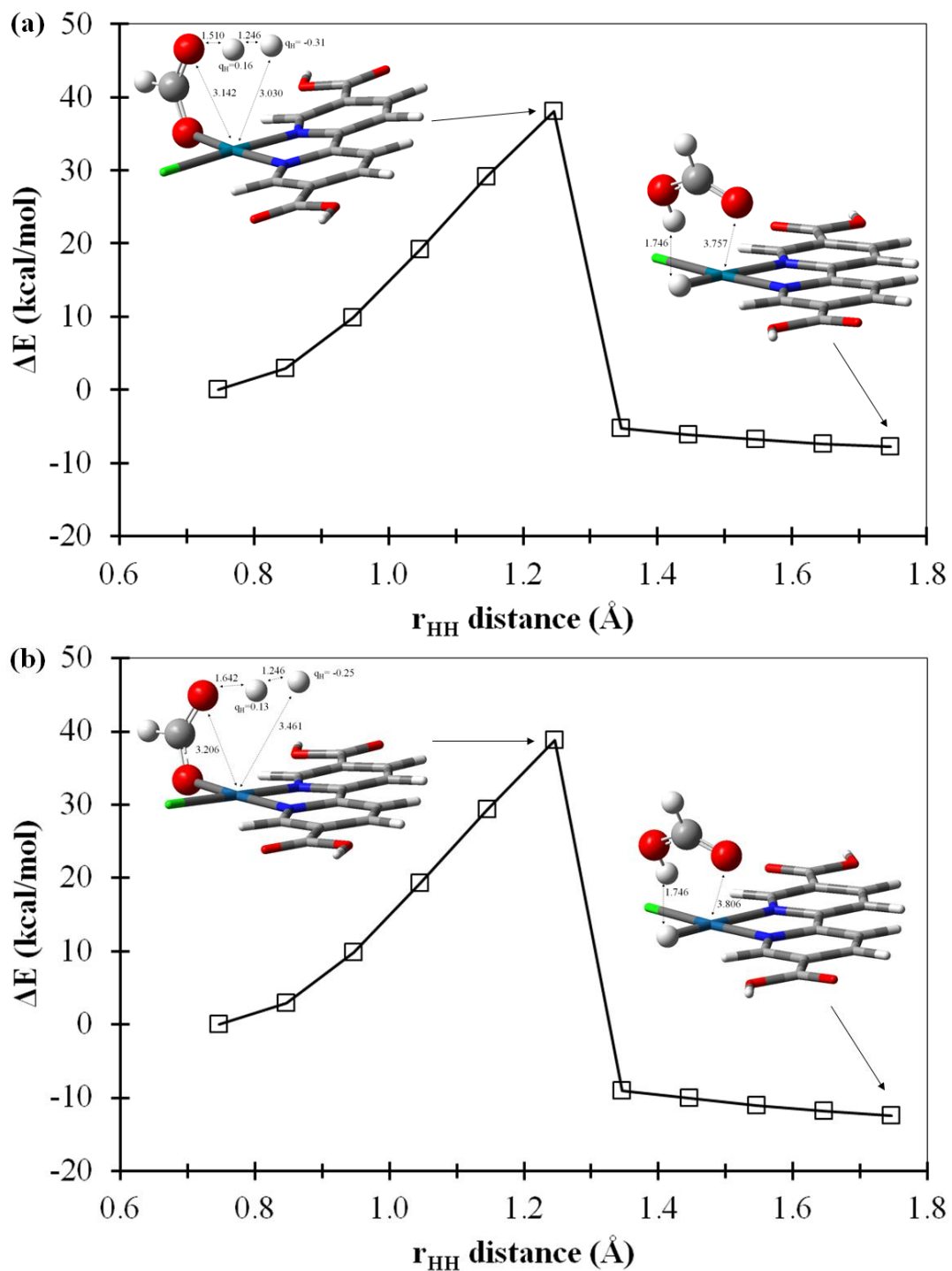


Figure S5. The calculated energetics of constrained optimization along H–H interatomic distance of (a) LPdCl(HCO_2)(H_2) and (b) LPPtCl(HCO_2)(H_2) complexes. The qH notation represents the atomic charge predicted by Natural Population Analysis.

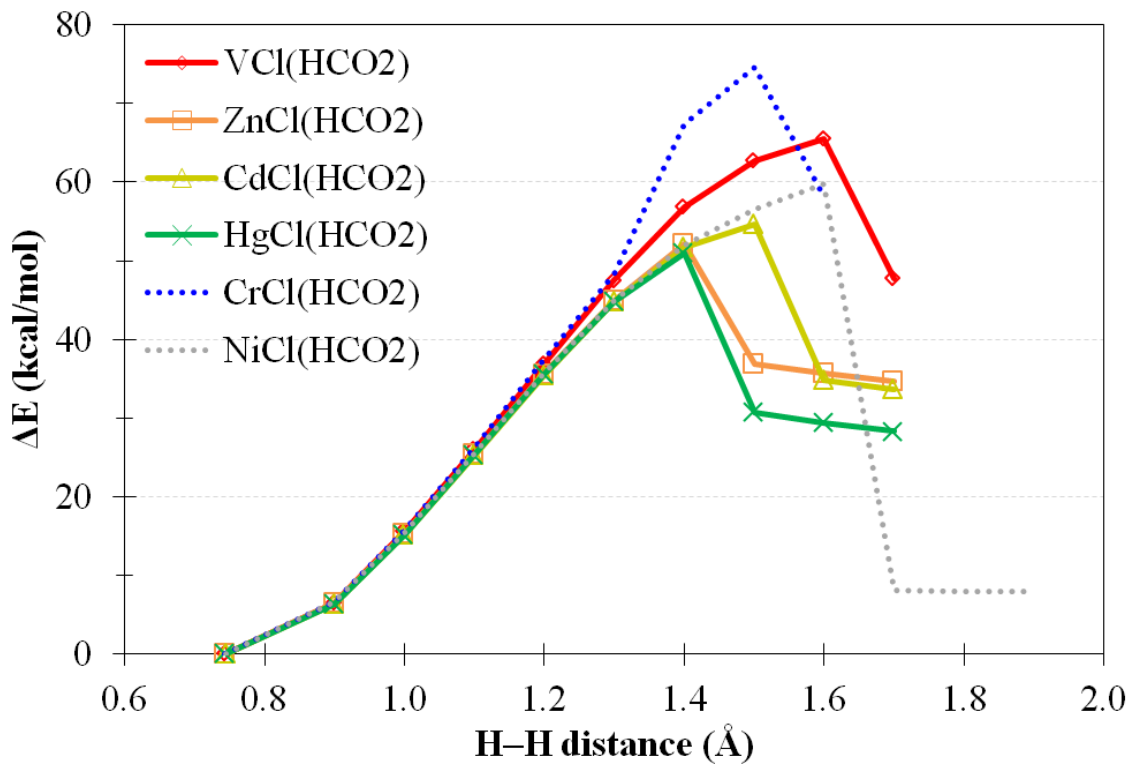


Figure S6. The schematic representation of H₂ activation by MCl(HCO₂), M = V, Zn, Cd, and Hg complexes. The solid lines denote the heterolytic H₂ activation pathways leading to the formation of HCOOH and Hbpy ligand as the H–H distances increase. The dotted lines denote non-physical reaction profiles for M = Cr (s=2/2) and Ni (s=0) cases.

Table S1. Various MCl_2 , $\text{M} = \text{Pd}$ and Sc , formation energetics (in eV) in MOF-253^{1,2}

Entry	Coordination	E_DFT	E _{tot}	E _{avg}
(1)	Pristine	-1555.74482		-
(2)	8PdCl ₂	-1648.67757	-30.8042	-3.85
(3)	7PdCl ₂	-1636.96451	-26.8572	-3.84
(4)	6PdCl ₂ _aa	-1625.20293	-22.8617	-3.81
(5)	6PdCl ₂ _ab	-1625.32115	-22.9799	-3.83
(6)	6PdCl ₂ _ac	-1625.22135	-22.8801	-3.81
(7)	6PdCl ₂ _bb	-1625.39509	-23.0538	-3.84
(8)	6PdCl ₂ _cc	-1625.29802	-22.9568	-3.83
(9)	8ScCl ₂	-1688.77110	-29.8151	-3.73
(10)	7ScCl ₂	-1672.07770	-26.1225	-3.73
(11)	4ScCl ₂	-1672.17710	-14.8299	-3.71

1. E_{tot} denotes the total binding energy of $n^*\text{MCl}_2$ in MOF-253, being expressed $E_{\text{tot}} = E_{\text{MOF-}n\text{M}} - E_{\text{MOF}} - n^*E_{\text{MCl}_2}$ where $E_{\text{MOF-}n\text{M}}$ and E_{MOF} represent the energy of MOF with or without the adsorbates, respectively.
2. E_{avg} denotes the average adsorption energy of MCl_2 in MOF-253 as $E_{\text{ads}} = E_{\text{tot}} / n - E_{\text{MCl}_2}$ where E_{MCl_2} represents the single gaseous molecule. E_{PdCl_2} is -7.76607 eV and E_{ScCl_2} is -12.90140 eV.

Table S2. Calculated structural information of MOF-253 upon PdCl₂ coordination¹

Adsorbates	$\angle \text{Al-O-Al}'$	$\phi(\text{Pd})$	$\phi(\text{w/o Pd})$	τ_{linker} (w/o PdCl ₂)	τ_{linker} (with PdCl ₂)
Pristine	131.80		97.16	7.27	
8PdCl ₂	132.16	97.30			23.84
7PdCl ₂	132.00	97.15	98.23	11.62	24.46
6PdCl ₂ _aa	132.01	96.98	97.92	8.45	26.06
6PdCl ₂ _ab	131.97	97.32	96.92	2.69	26.06
6PdCl ₂ _ac	131.99	96.38	98.18	12.15	24.54
6PdCl ₂ _bb	131.77	97.53	97.22	12.14	26.15
6PdCl ₂ _cc	131.88	96.86	97.27	4.37	25.97

1. The dihedral angles of linker-Al-Al'-linker' shown in Figure 1d are labelled as $\phi(\text{Pd})$ and $\phi(\text{w/o Pd})$ for the cases with or without PdCl₂ coordination, respectively.

Table S3. The labels of the spin states of $\text{LMCl}_2(\text{H}_2)$ intermediates¹

spins	Low Spin (LS)	High Spin (HS)	Medium Spin (MS)
$\text{LScCl}_2(\text{H}_2)$	1/2	X	X
$\text{LTiCl}_2(\text{H}_2)$	0	1	X
$\text{LVCl}_2(\text{H}_2)$	1/2	3/2	X
$\text{LCrCl}_2(\text{H}_2)$	0	2	1
$\text{LMnCl}_2(\text{H}_2)$	1/2	5/2	3/2
$\text{LFeCl}_2(\text{H}_2)$	0	2	1
$\text{LCoCl}_2(\text{H}_2)$	1/2	3/2	X
$\text{LNiCl}_2(\text{H}_2)$	0	1	X
$\text{LCuCl}_2(\text{H}_2)$	1/2	X	X
$\text{LZnCl}_2(\text{H}_2)$	0	X	X
$\text{LYCl}_2(\text{H}_2)$	1/2	X	X
$\text{LZrCl}_2(\text{H}_2)$	0	1	X
$\text{LNbCl}_2(\text{H}_2)$	1/2	3/2	X
$\text{LMoCl}_2(\text{H}_2)$	0	2	1
$\text{LTcCl}_2(\text{H}_2)$	1/2	5/2	3/2
$\text{LRuCl}_2(\text{H}_2)$	0	2	1
$\text{LRhCl}_2(\text{H}_2)$	1/2	3/2	X
$\text{LPdCl}_2(\text{H}_2)$	0	1	X
$\text{LAGCl}_2(\text{H}_2)$	1/2	X	X
$\text{LCdCl}_2(\text{H}_2)$	0	X	X
$\text{LTaCl}_2(\text{H}_2)$	1/2	3/2	X
$\text{LWCl}_2(\text{H}_2)$	0	2	1
$\text{LReCl}_2(\text{H}_2)$	1/2	5/2	3/2
$\text{LOsCl}_2(\text{H}_2)$	0	2	1
$\text{LIrCl}_2(\text{H}_2)$	1/2	3/2	X
$\text{LPtCl}_2(\text{H}_2)$	0	1	X
$\text{LAuCl}_2(\text{H}_2)$	1/2	X	X
$\text{LHgCl}_2(\text{H}_2)$	0	X	X

¹ X denotes the corresponding spin state is not taken into account in this study.

Table S4. The H–H bond lengths (\AA) of the optimized 6-coordinated $\text{LMCl}_2(\text{H})_2$ intermediates ¹

spins	LS	HS	MS
$\text{LScCl}_2(\text{H})_2$	1.869		
$\text{LTiCl}_2(\text{H})_2$			
$\text{LVCl}_2(\text{H})_2$			
$\text{LCrCl}_2(\text{H})_2$			
$\text{LMnCl}_2(\text{H})_2$		1.835	1.820
$\text{LFeCl}_2(\text{H})_2$	0.775		
$\text{LCoCl}_2(\text{H})_2$			
$\text{LNiCl}_2(\text{H})_2$	1.787		
$\text{LCuCl}_2(\text{H})_2$			
$\text{LZnCl}_2(\text{H})_2$			
$\text{LYCl}_2(\text{H})_2$			
$\text{LZrCl}_2(\text{H})_2$	2.552		
$\text{LNbCl}_2(\text{H})_2$	2.839		
$\text{LMoCl}_2(\text{H})_2$	2.024		1.683
$\text{LTcCl}_2(\text{H})_2$	1.558	1.945	2.042
$\text{LRuCl}_2(\text{H})_2$	0.820	1.819	1.720
$\text{LRhCl}_2(\text{H})_2$	0.804	1.532	
$\text{LPdCl}_2(\text{H})_2$	0.780	1.806	
$\text{LAgCl}_2(\text{H})_2$			
$\text{LCdCl}_2(\text{H})_2$			
$\text{LTaCl}_2(\text{H})_2$	2.761	0.780	
$\text{LWCl}_2(\text{H})_2$	2.647	0.771	1.896
$\text{LReCl}_2(\text{H})_2$	1.765	2.168	2.195
$\text{LOsCl}_2(\text{H})_2$	1.739	1.994	1.920
$\text{LIrCl}_2(\text{H})_2$	1.950	1.862	
$\text{LPtCl}_2(\text{H})_2$	2.099	2.064	
$\text{LAuCl}_2(\text{H})_2$			
$\text{LHgCl}_2(\text{H})_2$			

¹ The blank cells represent that the stable dihydrido intermediates cannot be identified where the criteria of inter-hydrogen distance is greater than 0.75 \AA .

Table S5. The H–H bond lengths (\AA) of the optimized 5-coordinated $\text{LMCl}(\text{H})_2$ intermediates ¹

spins	LS	HS	MS
$\text{LScCl}(\text{H})_2$	2.949		
$\text{LTiCl}(\text{H})_2$	2.157		
$\text{LVCl}(\text{H})_2$	1.801	1.844	
$\text{LCrCl}(\text{H})_2$	2.678	3.342	
$\text{LMnCl}(\text{H})_2$	0.814		0.784
$\text{LFeCl}(\text{H})_2$		0.777	
$\text{LCoCl}(\text{H})_2$	1.857		
$\text{LNiCl}(\text{H})_2$			
$\text{LCuCl}(\text{H})_2$			
$\text{LZnCl}(\text{H})_2$	1.900		
$\text{LYCl}(\text{H})_2$	3.338		
$\text{LZrCl}(\text{H})_2$	3.090		
$\text{LNbCl}(\text{H})_2$	2.232	2.162	
$\text{LMoCl}(\text{H})_2$	1.808	1.879	
$\text{LTcCl}(\text{H})_2$	2.742	1.752	2.692
$\text{LRuCl}(\text{H})_2$	2.126	1.985	
$\text{LRhCl}(\text{H})_2$	1.960	0.807	
$\text{LPdCl}(\text{H})_2$	1.757		
$\text{LAgCl}(\text{H})_2$			
$\text{LCdCl}(\text{H})_2$	2.101		
$\text{LTaCl}(\text{H})_2$	2.969	2.971	
$\text{LWCl}(\text{H})_2$	2.872	2.859	
$\text{LReCl}(\text{H})_2$	1.813	2.007	1.935
$\text{LOsCl}(\text{H})_2$	2.172	1.913	
$\text{LIrCl}(\text{H})_2$	2.048	1.564	
$\text{LPtCl}(\text{H})_2$	1.624		
$\text{LAuCl}(\text{H})_2$	2.045		
$\text{LHgCl}(\text{H})_2$	2.618		

¹ The blank cells represent that the stable dihydrido intermediates cannot be identified where the criteria of inter-hydrogen distance is greater than 0.75 \AA .